

## MINIREVIEW

[View Article Online](#)  
[View Journal](#) | [View Issue](#)Cite this: *Nanoscale Adv.*, 2021, 3, 6027

## Recent advances in peptide-based nanomaterials for targeting hypoxia

Jun Wang, \* Jing Liu† and Zhongxing Yang

Hypoxia is a prominent feature of many severe diseases such as malignant tumors, ischemic strokes, and rheumatoid arthritis. The lack of oxygen has a paramount impact on angiogenesis, invasion, metastasis, and chemotherapy resistance. The potential of hypoxia as a therapeutic target has been increasingly recognized over the last decade. In order to treat these disease states, peptides have been extensively investigated due to their advantages in safety, target specificity, and tumor penetrability. Peptides can overcome difficulties such as low drug/energy delivery efficiency, hypoxia-induced drug resistance, and tumor nonspecificity. There are three main strategies for targeting hypoxia through peptide-based nanomaterials: (i) using peptide ligands to target cellular environments unique to hypoxic conditions, such as cell surface receptors that are upregulated in cells under hypoxic conditions, (ii) utilizing peptide linkers sensitive to the hypoxic microenvironment that can be cleaved to release therapeutic or diagnostic payloads, and (iii) a combination of the above where targeting peptides will localize the system to a hypoxic environment for it to be selectively cleaved to release its payload, forming a dual-targeting system. This review focuses on recent developments in the design and construction of novel peptide-based hypoxia-targeting nanomaterials, followed by their mechanisms and potential applications in diagnosis and treatment of hypoxic diseases. In addition, we address challenges and prospects of how peptide-based hypoxia-targeting nanomaterials can achieve a wider range of clinical applications.

Received 20th August 2021  
Accepted 1st September 2021

DOI: 10.1039/d1na00637a

[rsc.li/nanoscale-advances](http://rsc.li/nanoscale-advances)

## 1. Introduction

Hypoxia is one of the most prominent features of solid tumors.<sup>1</sup> The uncontrolled growth and proliferation of tumors consume both nutrition and oxygen, resulting in both an unmet demand for oxygen and compromised delivery of oxygen to other parts of the body. The proliferation of tumor cells stimulates the generation of blood vessels; however, these vessels are abnormal in terms of both their macro- and micro-structure, leading to challenges in regulating the delivery of oxygen.<sup>2</sup> The tumor hypoxic microenvironment directly induces healthy cell apoptosis or necrosis and promotes tumor cell progression by upregulating related pathways including growth-factor signalling, tissue infiltration, metastasis, and genomic instability.<sup>3</sup> Hypoxia is related to the degree of malignancy, invasion, and prognosis of a tumor, as well as resistance to radiotherapy and chemotherapy, with higher degrees of hypoxia in tumors decreasing therapeutic response.<sup>4,5</sup> For some anticancer drugs, oxygen increases the cytotoxicity of the cell damage they cause. Therefore, hypoxia has become the main target of cancer treatment in tumor progression as well as a significant challenge to overcome in the development of new therapies that do not result in resistance to treatment.<sup>6</sup>

Peptides are short oligomers formed by amino acid units connected *via* amide bonds.<sup>7</sup> They are important components of proteins and the causal agent of biological structure and function. Owing to their good compatibility with tissues, cells, and other biological components, peptides are incredibly biocompatible and biodegradable, increasing their advantages for biomedical applications.<sup>8</sup> The ability to change the amino acid side chains allows for precise tuning of the secondary and tertiary structures of peptides. This modification can lead to increased cell penetration, increased payload retention, or self-assembling functionality. These secondary structures, which include  $\alpha$ -helices and  $\beta$ -sheets, can also cause interactions between peptide chains.<sup>9</sup> The interactions of secondary structures can lead to peptides forming nanostructures, such as nanofibers and micelles, which allows for increased cell penetration and large surface area to enable conjugation of the drug and imaging agent. In addition, the formation of these peptides can be triggered under certain conditions, allowing for flexibility and control. Peptide-based materials have been developed as unique and promising tools for the treatment of diseases. They have a variety of activities, including drug delivery, sensing, cell targeting, deep penetration of tissues, and immune responses to enhance anti-tumor treatment effects.<sup>10–12</sup> By combining several functionalities such as responsive cleavage sites, cellular targeting, endocytosis transporters, and

School of Pharmacy, Jining Medical University, Rizhao, 276800, China

† These authors contributed equally.





Table 1 Peptide-based hypoxia-targeting nanomaterials and their targeting strategies

Hypoxia-targeting strategies	Hypoxia-responsive motif	Peptide agent	Structures of nanomaterial/loaded agents	Results under hypoxic conditions	Ref.
Hypoxia-responsive motif	NI	Poly-glutamic acid	Nanoparticles/DOX	Shown faster release	32
		Poly-aspartic acid	Micelles/(Dox + Ce6)	Enhanced chemotherapy and PDT efficacy	34
		Poly-aspartic acid	Vesicles/insulin	Enhanced glucose responsive insulin delivery	35
		Poly-glutamide	Nanoparticles/siRNA	Silencing hypoxia-correlated pro-tumorigenic gene and significant suppression of tumor growth	36
	NA	Poly-lysine	Micelles/DOX	Enhanced tumor penetration and improved anti-tumor efficacy	37
	Azo	Poly-glutamate	Nanoparticles/DOX	Enhanced DOX release and superior tumor cell-killing ability	38
		Poly-aspartic acid	Micelles/cytochrome C	Shown great killing effect on HepG2 liver cancer cells	39
	NP	Poly-aspartic acid	Micelles/Ce6	Enhanced antitumor PDT efficacy	42
		Poly-lysine&AVPI-NP-C12	Nanofibers	Released a pro-apoptotic AVPI peptide	52
	Cy7	Surfactin	Nanoparticles/gambogic acid	Enhanced tumor localization, excellent biodistribution, and superior therapeutic efficacy	54
Hypoxia-responsive motif and peptide ligands	Azo	iRGD	Polymersomes/gemcitabine	Enhanced ability to target, penetrate and deliver drugs	68 and 86
	Azo	iRGD	Nanoparticles/DOX	Significantly diminished tumor growth	69
Peptide ligands	Azo	TAT peptide	Nanoparticles/Ce6+TPZ	Enhanced PDT and bio-reductive chemotherapy efficiency	71
	Azo	CRGDK	Nanoparticles/IR-780 + PFOB	Alleviated hypoxia and improved PDT efficiency	72
		(D)-Phe-(D)-Phe-(D)-Lys-OH	Nanofibers/DOX	Sensitized tumors to DOX administration and expedited conventional chemotherapy	59
		CCGKRTRGC	Nanoparticles/radiolabeled with <sup>131</sup> I	Improved local hypoxia and significantly inhibited tumor growth and metastasis	73
		iVR1 peptide	Nanoparticles/salidroside + apatinib	Inhibited tumor growth and metastasis	74
		cRGD	Liposomes/Ce6 + TPZ + ICG	Shown stronger anti-tumor effect	
		iRGD	Nanoparticles/TPZ + ICG	Enhanced the tumor therapeutic effect by the combination of PTT, PDT and chemotherapy	87
		GGGGDRVYHPF	Liposomes/BDP-NO <sub>2</sub>	Effectively inhibited primary tumor growth and metastasis	88
		Cyclopeptide RA-V	Liposomes/RX-0047+ anti-DR5	Could be used for real-time imaging of hypoxia levels of myocardial ischemia	93
		YPHDSLGHWRR	Hydrogel	Enhance the chemotherapy efficacy and achieved therapeutic self-monitoring	94
		TAT peptide	Nanoparticles/siRNAs	Enhanced cell survival, proliferation, and migration and improved cardiac repair	95
		RGD	Nanoparticles/HIF-1α-AA	Effectively inhibited tumor growth and angiogenesis	105
				Promoted angiogenesis and improved the recovery of nerve function	107

therapeutic activities, peptides can also be used as components of functionalized composite materials.<sup>13–15</sup>

There are three main ways through which these peptides have been used in the treatment of hypoxia-related diseases. The first is through utilizing a targeting ligand for therapy, usually involving targeting a specific cell, tissue, or microenvironment for the peptides' intended effect, with a majority of these strategies being where the peptide itself is the targeting ligand.<sup>16,17</sup> These strategies usually involve a cytotoxic small molecular peptide that has a method of selecting the target over non-target cells, and will either induce cytotoxic effects or provide protection from harmful external stimuli, such as hypoxia. The second method involves utilization of hypoxic sensitive linkers that can allow hypoxia triggered delivery of therapeutic or imaging payloads. The pathological environment of hypoxia increases reductive stress, leading to overexpression of different bio-reductases including nitroreductase (NTR), azoreductase (AZR), and quinone reductase.<sup>18,19</sup> Under hypoxic conditions, the reducible functional groups, including nitro, azo, and quinone, located on small molecules present in the cellular environment can accept electrons and be reduced.<sup>20</sup> With the reduction of these hypoxia-responsive moieties, the physicochemical properties and functions of the nanosystem can be changed, such as particle size, fluorescence, and hydrophilicity. Utilizing this information, significant improvements in nanotechnology have occurred by incorporating hypoxia-sensitive moieties, such as nitroimidazole (NI),<sup>21</sup> nitrobenzyl alcohol (NA),<sup>22,23</sup> and azobenzene (Azo)<sup>24</sup> derivatives to achieve the response to bio-reductase in hypoxic tissues.<sup>25</sup> Peptides can be conjugated to either imaging agents or therapeutics through the use of stimuli-responsive elements that will allow release of payloads in a specific environment into the targeted tissue. The third possible method where peptides are used involves a combination of the above strategies.<sup>26</sup> This involves a targeting motif of some type, allowing fewer non-target effects to occur, improving the effective dose, and enabling more complete imaging of hard to image areas. Peptides are ideal in these three strategies as they can be highly specific, making them ideal targeting agents, while also being biodegradable, allowing for clearance or recycling from the body.

In this review, we will focus on novel peptide-based functional nanomaterials containing hypoxia-responsive functional groups as well as hypoxia-targeting nanomaterials. We will explore how these groups can be further utilized with peptides in order to increase biocompatibility, lower the toxicity, and improve the effectiveness of existing imaging and cytotoxic drugs. In addition, we will discuss the various ways in which these peptides can act alone to produce their intended effects. Using multiple models of peptides including small molecular peptides, self-assembling peptides, polypeptides, peptide-polymer conjugates, and peptides functionalized to either liposomes or polysaccharides, we hope to illustrate the ways through which these systems can overcome common difficulties inherent to hypoxic diseases. Here, a series of peptide-based hypoxia-targeting nanomaterials and their targeting strategies are listed in Table 1.

## 2. Polypeptides

Polypeptides are a kind of biomedical polymer with  $\alpha$ -amino acid structural units.<sup>27</sup> Compared with traditional synthetic polymers, polypeptides allow for control of polarity and charge and also show stability against hydrolysis, are easily synthesized, and are biodegradable by enzymes *in vivo*. These protein-mimicking polymers inherit many properties of proteins, such as biocompatibility, versatility, bioactivity, and hierarchical assembly properties.<sup>28–30</sup> In addition, the combination of polypeptides and synthetic polymers can enhance solubility, processability, and antifouling properties, which greatly broadens the application of biological materials.<sup>31</sup> Introducing a hypoxia-responsive moiety (such as NI, Azo, or NA) into the side chain of the polypeptide can enhance the micellization, encapsulation of hydrophobic drugs, and hypoxia responsiveness due to its hydrophobic effect, resulting in selective drug release at the hypoxic regions.

Many polypeptides containing hypoxia-responsive NI motifs have been reported in drug delivery and tumor therapy.<sup>32–34</sup> For example, Yu *et al.* developed novel hypoxia and H<sub>2</sub>O<sub>2</sub> dual-sensitive polymersome-based vesicles (d-GRPs) for enhanced glucose-responsive insulin delivery. The vesicles were self-assembled by a diblock copolymer consisting of PEG and NI-modified polyserine linked by thioether (PEG-poly(Ser-S-NI)), which could encapsulate recombinant human insulin and glucose oxidase. In the process of the enzymatic conversion of glucose to gluconic acid, a local hypoxic environment was generated quickly, which promoted the biological reduction of NI to hydrophilic 2-aminoimidazoles. Meanwhile, the thioether moiety in the polymer eliminated the excess H<sub>2</sub>O<sub>2</sub> and promoted the disassembly of vesicles, releasing the encapsulated insulin. The glucose-responsive polymersomes could be further integrated with a painless microneedle-array patch platform for insulin delivery (Fig. 1).<sup>35</sup> Shi and co-workers developed a hypoxia-responsive nanoparticle consisting of NI-modified polypeptide methoxy poly(ethylene glycol)-*block*-poly(L-glutamide-*graft*-2-nitroimidazole) (mPEG-*b*-(PLG-*g*-NI)) and a cationic lipid-like compound, used to deliver siRNA to silence cell division cycle 20 gene (CDC20) expression in breast cancer cells. The delivery nanosystem showed prolonged blood circulation, high tumor accumulation, efficient CDC20 silencing, and high potent antitumor efficacy.<sup>36</sup>

Hypoxia-responsive polypeptides based on nitrobenzyl alcohol derivatives (NADs) are commonly found in the literature. One example of these, investigated by Park and co-workers, involved preparing hypoxia-responsive polymeric micelles formed by an amphiphilic *block* copolymer, poly(ethylene glycol)-poly( $\epsilon$ -(4-nitro)benzyloxycarbonyl-L-lysine) (PEG-*b*-PLys-*g*-NBCF).<sup>22</sup> The copolymer can self-assemble into micelles and encapsulate doxorubicin (DOX) under aqueous conditions. Under hypoxic conditions, the DOX-loaded micelles tend to be highly unstable and easily degraded by a 1,6-elimination reaction, resulting in rapid intracellular release of DOX. Similarly, the Shi group developed a complex micelle containing an NA motif which was prepared by co-assembly of poly( $\epsilon$ -



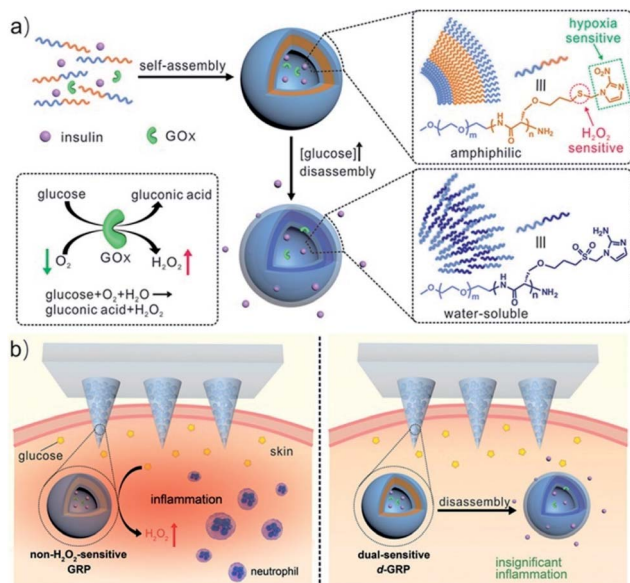


**Fig. 1** Schematic of the glucose-responsive insulin delivery system using hypoxia and H<sub>2</sub>O<sub>2</sub> dual-sensitive polymersome-based vesicle (d-GRP) loaded microneedle-array patches. (a) Formation and mechanism of d-GRPs consisting of PEG-poly(Ser-S-NI). (b) Schematic of local inflammation induced by a non-H<sub>2</sub>O<sub>2</sub>-sensitive GRP-loaded microneedle-array patch, and schematic of a d-GRP-loaded microneedle-array patch for *in vivo* insulin delivery triggered by a hyperglycemic state for potential prevention of the long-term side effect associated with inflammation. Reproduced with permission from ref. 35, copyright © 2017, American Chemical Society.

caprolactone)-*block*-poly(ethylene glycol) (PCL-*b*-PEG) and poly( $\epsilon$ -caprolactone)-*block*-poly(L-lysine)-*graft*-4-nitrobenzyl chloroformate (PCL-*b*-PLL-*g*-NBCF). The micelle design includes a PCL core and a hypoxia-responsive shell (NBCF-modified PLL and PEG). This core-shell structure can inhibit rapid removal by the immune system in the process of blood circulation. Once these micelles have reached the tumor site, the NBCF-modified PLL can degrade under the hypoxic micro-environment, leading to the increase of positively charged PLL on the surface of the micelles, enabling the penetration of the micelles into the tumor. In addition, *in vitro* and *in vivo* experiments show that these DOX-loaded micelles have better penetration ability and inhibitory effects on tumor tissues.<sup>37</sup> In another example, Zhang *et al.* synthesized a hypoxia-responsive polymer, mPEG-PLG-NC, by conjugating hydrophobic 4-nitrobenzyl (3-azidopropyl) carbamate (AP-NC) to the side chains of methoxy poly(ethylene glycol)-*b*-poly( $\gamma$ -propargyl-L-glutamate) (mPEG-PPLG) copolymers (Fig. 2). The polymer self-assembled into nanoparticles in aqueous solution and could load DOX with a high encapsulation efficiency of 97.8% due to the strong  $\pi$ - $\pi$  interaction between the *p*-nitrobenzyl group and DOX. The DOX-loaded nanoparticles (PPGN@DOX) showed hypoxia-responsive drug release behavior *in vitro*. PPGN@DOX can be effectively internalized by 4T1 cells and release DOX into the cell nucleus in a hypoxic environment. In addition, since PPGN@DOX provided a longer circulation time and improved the biodistribution of DOX, there were increased antitumor

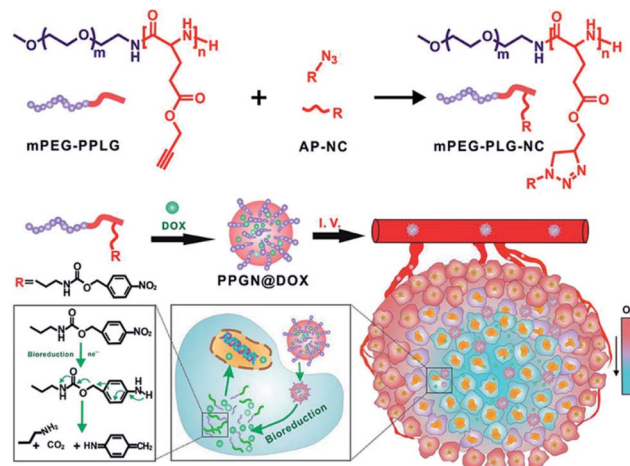


**Fig. 2** Schematic of the synthesis of mPEG-PLG-NC and preparation of PPGN@DOX for hypoxia-responsive drug delivery *in vivo*. Reproduced with permission from ref. 38, copyright © 2020 American Chemical Society.

outcomes and reduced side effects *in vivo*.<sup>38</sup> A further study with an NA modified hypoxia-sensitive polypeptide was carried out by Sun *et al.* who prepared polymeric micelles that were self-assembled by an amphiphilic polymer methoxy PEG-*block*-poly(diethylenetriamine-*graft*-4-nitrobenzyl chloroformate)-L-glutamate [mPEG-*b*-P(Deta-NBCF)LG] for the targeted delivery of metalloprotein cytochrome c (CC) to cancer cells. These CC-loaded micelles are effectively taken up by cancer cells and greatly enhance the cytotoxicity of CC to cancer cells under hypoxic conditions.<sup>39</sup>

Most nanocarriers consist of a steric PEG protective layer to maintain the stability of the system for protein adsorption.<sup>40</sup> However, the PEG layer usually hinders the cellular uptake of nanocarriers, resulting in the loss of photodynamic therapy (PDT) efficacy.<sup>41</sup> Designing a sheddable PEG (dePEGylation) is an effective means of balancing system stability and cellular uptake of nanocarriers. For this purpose, Li *et al.* reported hypoxia and singlet oxygen dually responsive multifunctional micelles to enhance antitumor PDT. The micelles were obtained by self-assembly of the amphiphilic methoxy poly(ethylene glycol)-azobenzene-poly(aspartic acid) copolymer conjugated with imidazole (IM) side chains (mPEG-Azo-PAsp-IM). Azo and IM are hypoxic and singlet oxygen-responsive (SR), respectively. Chlorin e6 (Ce6) could be efficiently loaded by the micelles as a model photosensitizer. The promotion of cellular uptake was achieved by triggering the collapse of Azo to cause the shedding of PEG. The oxidation of imidazole by the singlet oxygen decomposed the micelles and led to release of Ce6. In addition, singlet oxygen-mediated cargo release consumes oxygen and increases the degree of hypoxia, which in turn further improves cellular uptake of micelles (Fig. 3).<sup>42</sup>

Hypoxia-responsive amphiphilic *block* copolymers formed by polypeptides could assemble into nanocarriers with different morphologies, which were used for the controlled release of drugs under hypoxic conditions. Due to the passive targeting effect, these nanocarriers showed high tumor accumulation,



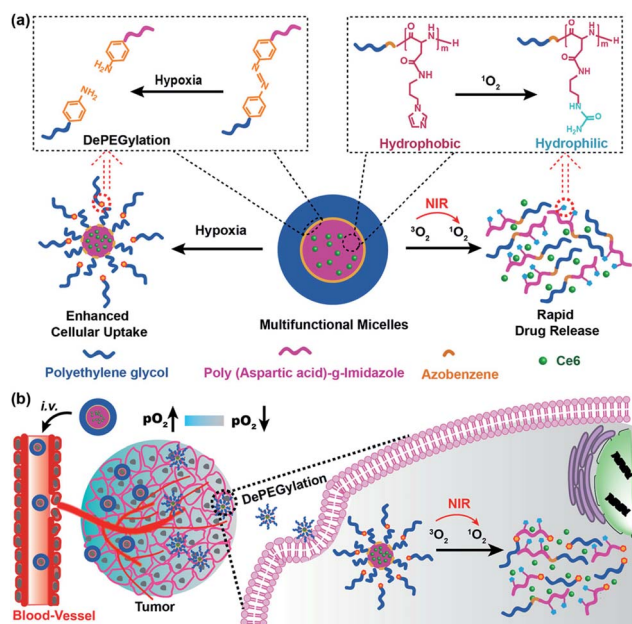


Fig. 3 Illustration of the interactively hypoxia- and singlet oxygen-sensitive tailor-made micelles for improved photodynamic antitumor therapy; (a) the hypoxia-responsive Azo linker was used to connect the hydrophilic PEG block and hydrophobic polypeptide block, producing a self-assembling amphiphilic copolymer; Ce6 was the model photosensitizer; the Azo and imidazole moieties are hypoxia- and SR moieties, respectively; (b) upon micelles reaching the tumor, the hypoxia-sensitivity would enable the DePEGylation and enhanced cellular uptake of micelles, while the singlet oxygen-responsiveness could lead to micelle disassembly and rapid Ce6 release. Reproduced with permission from ref. 42, copyright © 2018, American Chemical Society.

better penetration ability, and improved inhibition efficacy on tumor tissues. Therefore, these polypeptide-based hypoxia-targeting nanosystems present a promising and advanced strategy for precision cancer therapy.

### 3. Self-assembled peptides

Self-assembled peptides can spontaneously construct a series of well-defined supramolecular nanostructures, such as nanotubes, nanofibers, vesicles, and hydrogels.<sup>43</sup> Non-covalent interactions including hydrogen bonding, van der Waals interaction, electrostatic interaction, and hydrophobic effects maintain the self-assembled structure in a stable low-energy state.<sup>44</sup> The self-assembly of peptides can be effectively regulated by inherent or external stimuli such as pH, temperature, ionic strength, metal ion complexation, and enzymatic reactions.<sup>45–47</sup> Based on the characteristics of the individual self-assembled peptide, these nanostructures can have diverse applications in biomedicine, including drug delivery, tissue engineering, and regenerative medicine.<sup>48–50</sup>

The introduction of hypoxia-responsive motifs or targeting peptide ligands into the self-assembled peptide nanostructure can be used for the diagnosis and treatment of hypoxic diseases. An example is a study performed by Ikeda *et al.* who explored

pro-apoptotic peptide amphiphiles that could form self-assembled nanostructures.<sup>51</sup> The peptide amphiphile AVPI-NP-C12 was composed of a pro-apoptotic AVPI tetrapeptide connected with a hydrophobic dodecyl chain through a nitro-phenyl (NP) linker. In the presence of poly-L-lysine, AVPI-NP-C12 formed self-assembled nanostructures comprising entanglements of nanofibers. Mechanistically, the proposed theory for why this occurs is due to the electrostatic interaction between cations and the carboxylate anion of AVPI-NP-C12. Upon the addition of sodium dithionite, a reducing agent used to mimic the hypoxic environment, the NP motif can be reduced, leading to the decomposition of AVPI-NP-C12 and the release of a pro-apoptotic peptide. Apoptotic peptides can enhance the activity of anticancer drugs by inhibiting apoptosis protein inhibitors;<sup>52</sup> therefore, the nanostructures of pro-apoptotic self-assembling peptides have potential applications in nanomedicine for encapsulation and delivery of drugs, and sensing of hypoxic environments.

The charges of peptides can greatly affect the performance of the assembled nanostructures in nanomedicine. A negative charge can protect the nanostructures from being cleared before reaching the tumor tissue. However, due to the negative potential of the cytomembrane, the nanostructures are difficult to be engulfed by target cells.<sup>53</sup> Based on this concept, Wang *et al.* explored a selective-release “mosaic-type” nanoparticle, GA-Cy7-NP, for targeting hypoxic cancer cells. These nanoparticles were prepared by the self-assembly of surfactin, in addition to a single conjugate of heptamethine carbocyanine dye (Cy7) and gambogic acid (GA) in an aqueous solution. In this system, surfactin is used as a carrier platform, with Cy7 and GA being used as a hypoxia target group and antitumor drug, respectively. The Cy7 group is embedded in the surface of negatively charged nanoparticles formed by a surfactant, which enables these nanoparticles to selectively release the drug conjugates into hypoxic cancer cells without internalization of particles. GA-Cy7-NP also showed long-term circulation characteristics and high cell uptake in tumor cells. Compared with the prototype drug, it has stronger antitumor activity in cell proliferation, tumor growth, and angiogenesis.<sup>54</sup> Another example of using self-assembled peptides as drug delivery systems is the work of Zhu and co-workers who prepared an angiogenesis vessel-targeting nanoparticle (AVT-NP) containing photosensitizer 5-(4-carboxyphenyl)-10,15,20-trisphenylchlorin (TPC), angiogenesis vessel-targeting cyclopeptide (peptide sequence: CGNSNPKSC), and bio-reductive drug TPZ. Upon exposure to irradiation, the photosensitizer can generate large amounts of reactive oxygen species (ROS), which will reduce TPZ to form cytotoxic free radicals. *In vivo* experiments demonstrated that AVT-NP can specifically accumulate around tumor cells through the targeting of angiogenesis vessels. The system also exhibited enhanced antitumor efficiency with the chemo-photo synergistic effect.<sup>55</sup>

The intracellular self-assembly of nanomaterials shows a high retention rate and low cytotoxicity, which has great application potential in long-term tumor biological imaging.<sup>14</sup> Based on the strategies of intracellular transglutaminase (TG2) mediated catalytic polymerization and *in situ* self-assembly of



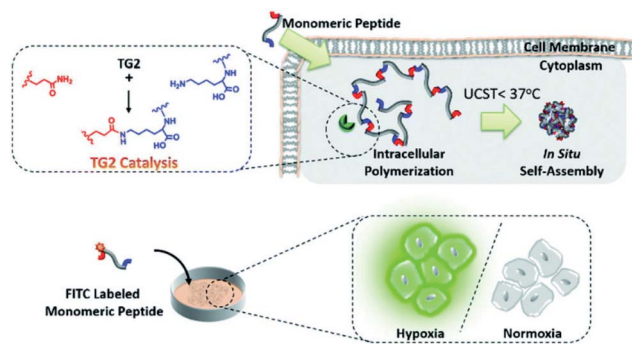


Fig. 4 Schematic illustration of specific transglutaminase 2 (TG2)-catalyzed intracellular polymerization, temperature induced *in situ* self-assembly and hypoxic neuroblastoma cell imaging. Reproduced with permission from ref. 56, copyright © 2020, Royal Society of Chemistry.

polymerized elastin-like polypeptides (ELPs), Li and co-workers reported a peptide-based probe for imaging hypoxic neuroblastoma cells. In this system, the polymeric monomer peptides are composed of N- and C-terminal amino acid polymeric active sites (e.g., Q and K) and elastin repeating units (XGVGP or GYGXP). To optimize TG2-catalyzed polymerization into ELPs, many parameters, namely peptide sequences, heat sensitivity, and the upper critical solution temperature (UCST), are studied to fine-tune the system for the maximum effect. In cells that overexpress TG2 (such as HeLa), intramolecular polymerization and self-assembly can enhance retention efficiency and intracellular accumulation. Due to the up-regulation of TG2 expression under hypoxia, FITC-labelled peptide probes can selectively image hypoxic neuroblastoma cells for diagnostic work (Fig. 4).<sup>56</sup>

Self-assembling peptides can be designed to form tunable supramolecular nanostructures triggered by targeted cellular environments.<sup>57</sup> These pericellular nanostructures provide effective strategies to change the interaction mechanism of enzymes with cells and promote or reduce their cellular uptakes.<sup>58</sup> Recently, Li *et al.* developed a self-assembling carbonic anhydrase (CA) inhibitor based on self-assembling peptides, which specifically interacted with the overexpressed CA on hypoxic cancer cell membranes. This complex boosted the inhibition and selectivity of the CA inhibitor through the strategy of hypoxia-triggered self-assembly. The self-assembling CA IX inhibitor N-pepABS was synthesized by conjugating a commercially available CA inhibitor, 4-(2-aminoethyl) benzenesulfonamide (ABS), with a self-assembled motif [2-naphthaleneacetic acid-(D)-Phe-(D)-Phe-(D)-Lys-OH (N-pep)]. N-pepABS can target CA IX and self-assemble into nanofibers, which enables CA IX inhibitors to concentrate on the membrane of hypoxic cancer cells, resulting in interruption of hypoxic cancer cells. These CA-triggered nanofibers promote cellular uptake through CA IX-mediated endocytosis. In the process of internalization, nanofibers may transform into larger nanofiber bundles under low pH conditions. The bundles will in turn cause damage to the intracellular acid vesicles and blockage of protective autophagy. These results provide

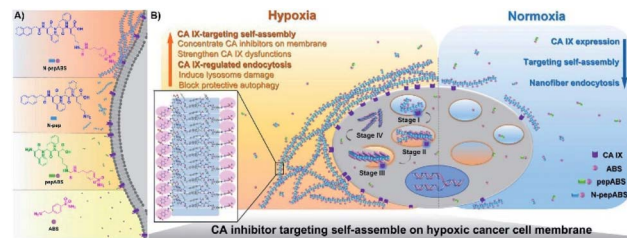


Fig. 5 Molecular design of self-assembled CA IX inhibitors (A) and their hypoxic cancer cell-targeted self-assembly (B). Adapted with permission from ref. 59, copyright © 2019 The Authors, some rights reserved; exclusive licensee American Association for the Advancement of Science.

evidence that the cell milieu-triggered tunable nanostructure produces highly selective toxicities to hypoxic cancer cells. Moreover, the antimetastatic and antiangiogenic functions of N-pepABS were evaluated in murine 4T1 breast cancer cells. N-pepABS efficiently decreased tumor volume and reduced the number of lung metastases. Upon the detection of endothelial marker CD31, the intact tumor vessels turned dissociative and were muted after treatment with N-pepABS. In addition, the combination therapy of N-pepABS and doxorubicin (Dox) showed that N-pepABS treatment can effectively make tumors sensitive to Dox administration and significantly enhance anti-tumor efficacy (Fig. 5).<sup>59</sup>

Based on the inherent biocompatibility and biodegradability, the bioinspired nanostructures originating from self-assembled peptides extraordinarily benefit tumor therapy. The versatility of tunable nanostructures responding to the cell milieu impressively provides strategic therapy for hypoxic tumors. In addition, self-assembly *in vivo* may be a potential nanotechnology in biomimetic structure fabrication *in vivo* in the future. Using peptide-based monomers for intracellular catalytic polymerization and assembly may provide a new strategy for hypoxic cancer therapy.

## 4. Peptide–polymer conjugates

Peptide–polymer conjugates are a kind of soft material formed by the covalent linkage of peptides and polymers. In these structures, polymer conjugation imparts processability to the peptides under different conditions (*i.e.*, solvent, temperature, and pressure), while the peptide imparts precision (*e.g.*, sequence control and low dispersity) to the peptide–polymer conjugates.<sup>60</sup> Due to their biocompatibility, biodegradability and mechanical strength, many polymers such as polylactic acid (PLA), polyglycolic acid (PGA), poly(lactic acid glycolic acid) (PLGA) and poly( $\epsilon$ -caprolactone) (PCL) combined with PEG have been widely used in peptide–polymer conjugate studies.<sup>61,62</sup> In addition, when tumor-targeting peptides are conjugated with these polymers, the affinity for the receptor, cell internalization, and tissue penetration ability can be enhanced.<sup>63–65</sup> Based on these characteristics, materials composed of peptide–polymer conjugates have a wide range of applications in biomedical sciences, such as drug delivery, tumor therapy, gene delivery, and antibacterial coatings.<sup>66,67</sup>



Recently there have been increasing studies on tumor hypoxia therapy utilizing peptide-polymer conjugates. One such design is centered on hypoxia-reactive motifs. An example of such a system is the work by Mallik and co-workers who developed tissue-penetrating, hypoxia-responsive polymersomes that could deliver the anticancer drug gemcitabine to solid tumors. The polymersomes are composed of a hypoxia-responsive Azo incorporated polylactic acid-polyethylene glycol (PLA-PEG) polymer and a tissue penetrating peptide iRGD (peptide sequence: CRGDKGPDC) functionalized PLA-PEG polymer. Drug-encapsulated polymersomes greatly reduced the viability of pancreatic cancer cells<sup>68</sup> and triple-negative breast cancer cells<sup>69</sup> in spherical cultures and successfully released the encapsulated contents *in vitro* and *in vivo* under hypoxic conditions. More research in this area by Ma *et al.* developed a novel AZR responsive nanoprobe (Micelle@Mito-rHP@TATp, MCM@TATp) for specific imaging of mitophagy in living cells under hypoxia by encapsulating mitochondria-targeted rhodamine spirolactam derivatives (Mito-rHP). The micelle MCM was formed by self-assembling of a hypoxia-responsive amphiphilic polymer, 1,2-distearoyl-*sn*-glycero-3-phosphoethanolamine-Azo-N-[maleimide(polyethylene glycol)2000] (DSPE-Azo-PEG-Mal), in aqueous solution and simultaneously encapsulating a rhodamine spirolactam derivative (Mito-rHP). Then MCM was functionalized by a cell-penetrating peptide (TATp, RKKRRQRRRC), which ensured that the nanoprobe could be transported into the cytoplasm in

a receptor-independent manner, thus avoiding the restriction of the nanoprobe in the endosome or lysosome. Under hypoxic conditions, the nanoprobe was disrupted by the highly expressed AZR. The encapsulated probe Mito-rHP was then released and able to target mitochondria. Because Mito-rHP is also pH-sensitive, it is converted into a protonated form during mitophagy, thus stimulating a fluorescent signal to switch from “off” to “on”.<sup>70</sup> Another study with the Azo motif was carried out by Jiang and co-workers who developed a hypoxia-responsive drug delivery system for combined PDT and bio-reductive chemotherapy. There, sensitive amphiphilic polymer monomethoxy PEG-azobenzene-PLGA (PEG-Azo-PLGA) was first synthesized and conjugated with TAT peptide (peptide sequence: YGRKKRRQRRRC-NH<sub>2</sub>) and 2,3-dimethylmaleic anhydride (DA) successively to obtain the polymer <sup>DA</sup>TAT-PEG-PLGA. After that nanoparticles <sup>TAT + Azo</sup>NPs were prepared by PEG-Azo-PLGA and <sup>DA</sup>TAT-PEG-PLGA. Due to the TAT peptide attached on the surface, <sup>TAT + Azo</sup>NPs can keep the cargoes Ce6 and TPZ and accumulate within tumor cells. Under laser irradiation, and with sufficient oxygen supply, <sup>TAT + Azo</sup>NPs achieved effective PDT on tumor cells proximal to vessels. Oxygen consumption during PDT further generated a hypoxic micro-environment, which could trigger the release of TPZ by breakage of the azobenzene bond, and accelerated the activation of TPZ, thereby improving the efficacy of combined treatment in tumor cells distal to the vessel (Fig. 6).<sup>71</sup>

Recently, Liu *et al.* reported reactive oxygen species (ROS) sensitive arylboronic ester-based nanocarriers modified with red blood cell membrane and iRGD peptide. These nanocarriers can be utilized for co-encapsulation of Ce6 and TPZ to achieve tumor specific release and synergistic PDT.<sup>65</sup> Similarly, Zhao *et al.* developed deep penetrating and oxygen self-sufficient PDT nanoparticles based on peptide-polymer conjugates, which were used to balance the distribution of ROS in tumors. These nanoparticles (CNP/IP) are prepared by the co-assembly of peptide (peptide sequence: CRGDK)-PEG-PCL and PEG-PCL and simultaneously encapsulating a photosensitizer, IR780, and an artificial blood substitute, perfluorooctyl bromide (PFOB), with higher oxygen storage capacity. Modification of CRGDK peptide on the nanoparticles greatly promoted the accumulation and penetration of the encapsulated IR780 and PFOB into the interior of the tumor. In hypoxic regions, PFOB released oxygen, effectively alleviating hypoxia and enhancing PDT efficacy.<sup>72</sup>

In another study, Song *et al.* developed a multifunctional platform composed of <sup>131</sup>I-labeled dendrimers modified with a LyP-1 (peptide sequence: CCGNKRTRGC (C2-C10)) peptide for targeted antitumor and antimetastasis therapy.<sup>73</sup> The nano-system was prepared by generation 5 (G5) poly(amidoamine) dendrimers conjugated with PEG-LyP-1 and 3-(4'-hydroxyphenyl)propionic acid-OSu (HPAO), and then the remaining dendrimers were acetylated and radiolabeled with <sup>131</sup>I. The <sup>131</sup>I-labeled LyP-1-modified dendrimers had promising biocompatibility and could be utilized as a diagnostic probe for single-photon emission computed tomography (SPECT) imaging. Meanwhile, the LyP-1 peptide could recognize tumor cells in hypoxic regions and relieve hypoxia, in addition to being used

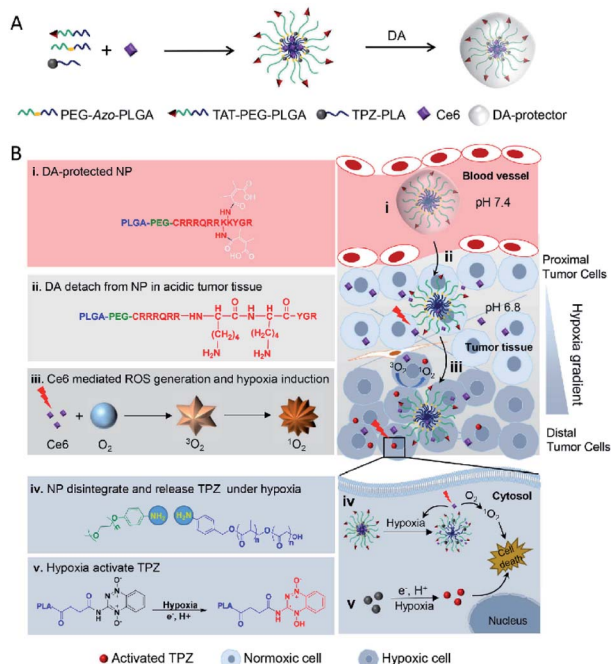


Fig. 6 Schematic illustration of tumoral pH activatable and hypoxia responsive NPs (<sup>TAT + Azo</sup>NPs) for enhancing PDT-induced hypoxia activated chemotherapy. (A) Fabrication of tumoral pH activatable and hypoxia responsive NPs. (B) Proposed mechanism of <sup>TAT + Azo</sup>NPs. <sup>TAT + Azo</sup>NPs followed multiple steps to meet ideal anticancer therapy. Reproduced with permission from ref. 71, copyright © 2020, Elsevier Ltd.

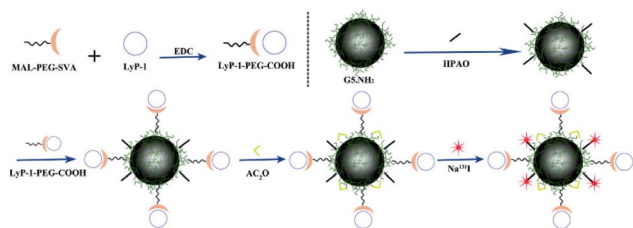


Fig. 7 Schematic diagram of the formation of G5.NHAc-HPAO-131I-(PEG-LyP-1). Reproduced with permission from ref. 73. Copyright © 2020, American Chemical Society.

as a carrier for anti-tumor and anti-metastatic therapy. The nanotheranostic system showed specific targeting *in vitro* and in tumor sites and could significantly inhibit tumor growth and metastasis *in vivo*, further providing evidence of its possible usefulness in therapy (Fig. 7).

A hypoxic microenvironment in solid tumors usually significantly reduces the chemosensitivity of cancer cells. Recent work by Zhang *et al.* developed a novel combined treatment strategy that can combat the drug resistance of gastric cancer *in vivo* and *in vitro*.<sup>74</sup> Salidroside (Sal) and apatite (Apa) were co-loaded by PLGA nanoparticles (NPs) to enhance the chemotherapy effect of apatinib on gastric cancer. To improve the drug delivery efficacy, the tumor recognizable peptide iVR1 was further modified on the NPs-Apa/Sal. iVR1 peptide can specifically target the vascular endothelial growth factor receptor 1 (VEGFR1) and inhibit angiogenesis and progression of certain cancers by selectively antagonizing VEGFR1.<sup>75</sup> The peptide-modified iVR1-NPs-Apa/Sal displayed excellent capability of tumor targeting drug delivery and showed an effective inhibitory effect on cell growth, invasion, and migration, as well as tumor progression *in vivo*. A mechanistic study showed that the enhancement of the chemotherapeutic effect of Apa was likely due to Sal inducing cell apoptosis and reprogramming the hypoxic tumor micro-environment.

In this section, nanocarriers formed by polymers modified with peptide ligands greatly facilitated the accumulation and penetration of the encapsulated contents into both the tumor periphery and hypoxic tumor inner regions. Such a strategy may have great potential in inhibiting tumor growth and metastasis, and could also have possible application in alleviating the hypoxia-induced chemotherapy resistance.

## 5. Peptide functionalized liposomes

Liposomes are phospholipid vesicles with a lipid bilayer structure and an inner aqueous compartment formed by self-assembly of amphiphilic molecules in water.<sup>76</sup> These structures can not only encapsulate the hydrophilic compound in their core, but also encapsulate the hydrophobic compound in the bilayer.<sup>77</sup> Due to their biocompatibility, self-assembly capacity, and the ability to direct passive targeting by enhancing the permeability and retention in the tumor area, liposomes are promising systems for drug and gene delivery, ophthalmology, vaccines, imaging, and cosmetics.<sup>78–80</sup>

Liposomes modified with a targeting peptide increase the targeting specificity and transfection efficiency in cells, and make nanocomplexes have better biocompatibility.<sup>81,82</sup> These peptide-liposomal systems targeting hypoxia for drug delivery,<sup>83</sup> gene delivery,<sup>84</sup> and cancer therapy<sup>85</sup> have been explored. Kulkarni *et al.* prepared liposomes composed of 1,2-distearoyl-*sn*-glycero-3-phosphocholine (DSPC), a hypoxia-responsive PEGylated lipid palmitoyl oleoylphosphatidylethanolamine (POPE)-Azo-PEG, and an iRGD peptide coupled lipid DSPE-PEG-iRGD. The iRGD peptide on the surface allowed liposomes to penetrate deeper and deliver the anticancer drug to the hypoxic cores. Under hypoxic conditions, the Azo moieties of the hypoxia-responsive lipids were reduced, which destroyed the stability of the lipid membrane and released the encapsulated drug from liposomes, resulting in increased cytotoxicity of the cultured pancreatic cancer cell.<sup>86</sup>

Liposome-based multiple responsive and multiple functional nanoplatforms for hypoxic tumor therapy have been reported. One such report by Dai *et al.* involved the preparation of a liposome *via* self-assembly of an amphiphilic molecule (mPEG-Ce6-C<sub>18</sub>), lecithin, and DSPE-PEG-cRGD (peptide sequence: RGD-D-FK). The liposome can encapsulate indocyanine green (ICG) and hypoxia-activated prodrug tirapazamine (TPZ), followed by chelation with Gd<sup>III</sup> to form a multifunctional theranostic liposome, ICG/TPZ@Ce6-Gd<sup>III</sup>. These multifunctional liposomes can be used not only as a multimodal imaging contrast agent but also as a PTT (photothermal therapy)-PDT (photodynamic therapy)-chemotherapy cascade activated antitumor agent. cRGD targeting and photothermally activated PDT can effectively minimize side effects on normal cells. Meanwhile, TPZ can enhance

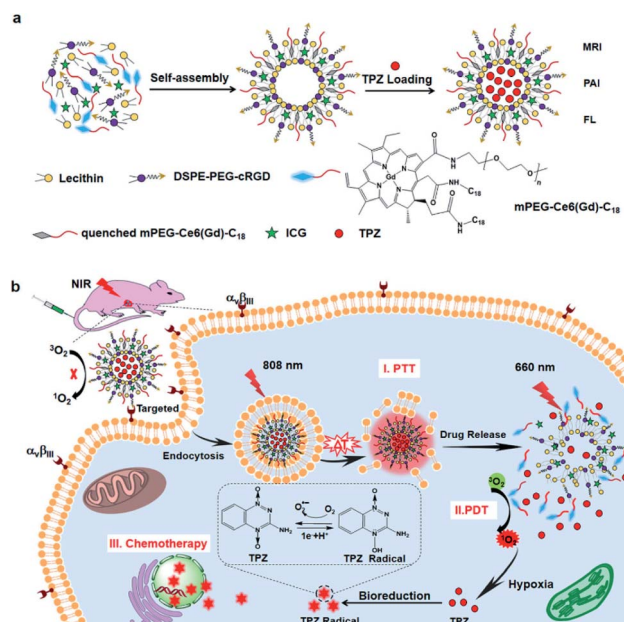


Fig. 8 Synthesis of ITC-Gd<sup>III</sup> TLs and NIR-triggered cascade-activated combination therapy. (a) Synthesis of ITC-Gd<sup>III</sup> TLs by self-assembly; (b) cascade-activated combination therapy for improved lung tumor therapeutic efficacy triggered by NIR light. Reproduced with permission from ref. 87. Copyright © 2019, American Chemical Society.



the therapeutic effect allowing this novel nanosystem to achieve the selective combination treatment of tumors (Fig. 8).<sup>87</sup> A similar synergetic mechanism was utilized by Wang *et al.* to achieve hypoxia-activated chemotherapy combined with PDT against metastatic breast cancer by simultaneously delivering ICG and TPZ to solid tumors through iRGD-modified liposomes.<sup>88</sup> In another study, You and co-workers proposed a dual endoplasmic reticulum (ER) targeting strategy to achieve PDT–PTT–immunotherapy. The nanosystem was composed of modified ER-targeting padaxin (FAL) peptides, ICG conjugated hollow gold nanospheres (FAL-ICG-HAuNs), and oxygen carrying HB liposomes (FAL-HB-lipo) for reversing hypoxia. Under NIR light irradiation, the ER-targeting nanosystem can induce strong ER stress and calreticulin (CRT) exposure on the cell surface. CRT exposure is a signal that stimulates the maturation of naive dendritic cells and induces an enhanced immune response, including CD8<sup>+</sup> T cell proliferation and cytotoxic cytokine secretion. ER-targeting PDT–PTT promotes immunotherapy associated with immunogenic cell death through direct ROS-based ER stress and exhibits enhanced antitumor efficacy.<sup>89</sup>

Utilizing the overexpression of several reductases under hypoxic conditions, many reductase fluorescent probes have been developed and successfully used for imaging the hypoxia status of tumor cells.<sup>90–92</sup> Recently, Fan *et al.* developed a liposome-based nanoprobe functionalized with a peptide (GGGGDRVYIHPF) to target cardiac cells and encapsulate them with nitrobenzene substituted BODIPY (BDP-NO<sub>2</sub>) for myocardial hypoxia imaging. Due to the peptide (GGGGDRVYIHPF), the system can specifically target the angiotensin II type 1 (AT1) receptor overexpressed on ischemic heart cells. The nanoprobe is taken up by the cardiac cells and releases BDP-NO<sub>2</sub>. Under hypoxic conditions, the nitro group of BDP-NO<sub>2</sub> is reduced to

BDP-NH<sub>2</sub> by NTR, resulting in a fluorescence enhancement of the nanoprobe. Furthermore, the nanoprobe can be used for real-time imaging of hypoxia levels in a mouse model of myocardial ischemia.<sup>93</sup> Yao *et al.* used real-time therapeutic monitoring to explore a combination therapy liposome nanosystem for high-efficiency therapy against hypoxic tumors and real-time imaging during apoptosis. In this study, a pH-sensitive liposome co-encapsulated a chemotherapeutic drug cyclopeptide RA-V (deoxybouvardin) and antisense oligonucleotides (RX-0047), as well as a caspase-8 probe. The obtained liposomes could selectively enter the lysosome of colon cancer cells through receptor-mediated endocytosis, and the lysosomal acidic microenvironment stimulated the liposomes to release the payloads. The released RA-V could induce apoptosis of cancer cells through the mitochondrial pathway, while the antisense oligonucleotides could inhibit the expression of HIF-1 $\alpha$  to alleviate tumor hypoxia. Moreover, the liposome can also be used for therapeutic self-monitoring through the fluorescence of the caspase-8 probe (Fig. 9).<sup>94</sup>

For a brief summary, nanosystems originating from peptide functionalized liposomes for targeting hypoxia have attracted more and more attention for the synergistic treatment of cancer. The introduction of hypoxia-responsive or other responsive motifs into the liposome structure will provide a new strategy for the design and development of multi-response, multifunctional therapeutic nanoplateforms.

## 6. Peptide functionalized polysaccharides

Polysaccharides are a kind of natural macromolecular polymer composed of long chains of monosaccharide units linked by glycosidic bonds.<sup>95</sup> As natural biomaterials, polysaccharides are generally regarded as water-soluble, safe, non-toxic, biodegradable, and nonimmunogenic, making them widely applicable in biomedicine.<sup>96,97</sup> In polysaccharides, hydrophilic functional groups such as the hydroxy group and carboxy group are easy to be chemically and biochemically modified and can also cause bioadhesion with biological tissues (mainly epithelium and mucosa) through non-covalent interactions. These nanocarriers made of bioadhesive polysaccharides can prolong the residence time in the mucosa, thus increasing the bioavailability of drugs. In addition, the surface of polysaccharide nanocarriers could be modified with ligands to actively target drug molecules.<sup>98</sup> In recent years, polysaccharide-based nanosystems for hypoxic tumor therapy have been developed,<sup>99–102</sup> among which peptide-functionalized polysaccharide nanomaterials have been reported, although research in this area is not as deep. An example is the work of Shu *et al.* who developed a RoY (peptide sequence: YPHIDSLGHWRR) peptide modified chitosan chloride hydrogel (CSCI-RoY). Using the targeting properties of RoY peptide, CSCI-RoY hydrogel can regulate the expression level of 78 kDa glucose-regulated protein (GRP78) receptor on the membrane of human umbilical vein endothelial cells, then activate protein kinase B (Akt) and extracellular signal-regulated kinase (ERK1/

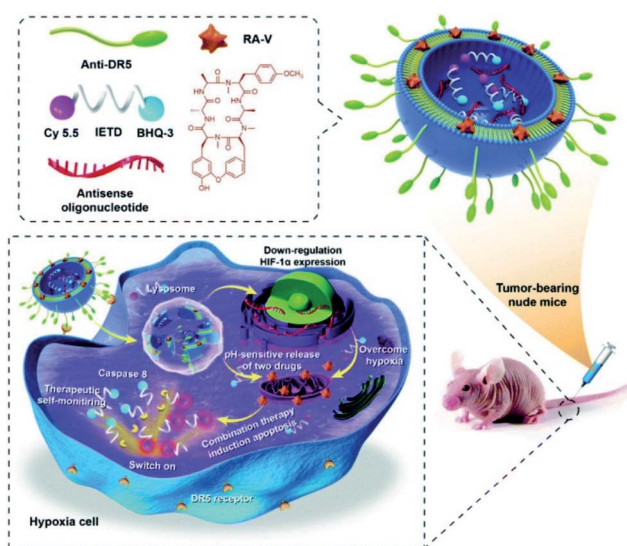
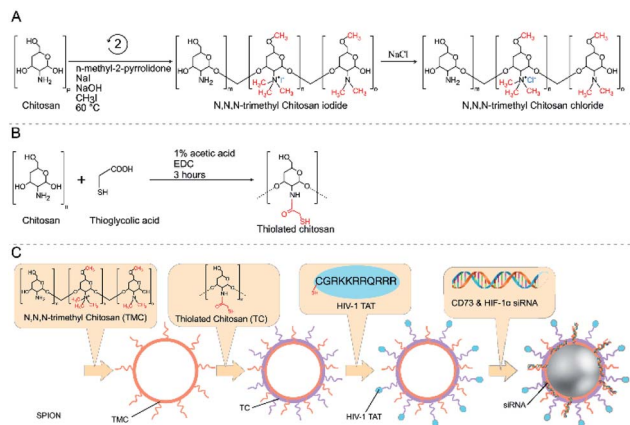


Fig. 9 Schematic illustration of co-delivery of cyclopeptide RA-V and antisense oligonucleotide with therapeutic self-monitoring in colon cancer. Reproduced with permission from ref. 94. Copyright 2020, Royal Society of Chemistry.



**Fig. 10** Reaction scheme for the synthesis of trimethyl chitosan and thiolated chitosan (A and B). Production of siRNA-loaded TAT-TMC-TC-SPION NPs (C). Reproduced with permission from ref. 105. Copyright 2020, © 2020 Elsevier B.V.

2) signaling pathways related to cell survival/proliferation, thereby enhancing cell survival, proliferation, migration and tube formation under hypoxic conditions. The study also demonstrated that the introduction of Roy peptide can not only induce angiogenesis at the infarct region but also improve cardiac repair.<sup>103</sup>

The CD73 molecule (ecto-5'-nucleotidase) is one of the molecules affected by hypoxia, as well as HIF-1 $\alpha$ , which plays a key role in the growth and spread of cancer.<sup>104</sup> Ghahmfarisa *et al.* developed a delivery system for silencing CD73 and HIF-1 $\alpha$  genes using superparamagnetic iron oxide (SPION) nanocarriers loaded with siRNA for cancer therapy (Fig. 10). In this nanosystem, siRNA-loaded SPIONs were encapsulated by thiolated chitosan (TC) and trimethyl chitosan (TMC) to improve their stability and functionality. The produced TMC-TC-SPIONs were conjugated with TAT peptide (C (Npys) GRKKRRQRRR) to increase the cellular uptake and form nanoparticles TAT-TMC-TCSPIONs. These nanoparticles could significantly reduce the expression of HIF-1 $\alpha$  and CD73 in cancer cells, resulting in a significant reduction in the migration and proliferation of cancer cells. In addition, *in vivo* evaluation showed that these nanoparticles could effectively inhibit tumor growth and angiogenesis (Fig. 10).<sup>105</sup>

A hyperbranched cationic amylopectin derivative conjugated with 3-(dimethylamino)-1-propylamine (DMAPA-Amyp) has good blood compatibility and low cytotoxicity, allowing it to be used as an effective gene carrier.<sup>106</sup> In a recent study by Deng *et al.*, an RGD (peptide sequence: KYGRGDC)-modified targeted gene nanocarrier, RGD-DMAPA-Amyp, for ischemic stroke treatment was synthesized. The targeting strategy was involved in the selection of RGD peptides, binding them to the nanocarriers and delivering them to the vascular endothelial cells in the peri-infarct region. The HIF-1 $\alpha$  mutant form (HIF-1 $\alpha$ -AA) was loaded with RGD-DMAPA-Amyp in the treatment of cerebral ischemia. The results demonstrated that this nanocomplex had good biocompatibility and could significantly improve the recovery of nerve function and the formation of new blood vessels *in vivo*.<sup>107</sup>

Because many polysaccharides have a high potential for binding to oligonucleotides, nanocarriers formed by peptide functionalized polysaccharides have been used as an effective targeted gene vector into hypoxic cells. These strategies can enhance the efficiency of gene transfection and the therapeutic effect of cancer or ischemic diseases.

## 7. Conclusion and future perspectives

In summary, utilizing the properties of the peptide system in diagnosis and treatment provides an opportunity to overcome the hurdles hypoxic diseases pose. As outlined, peptides have several advantages, including targeting specificity, tumor penetrability, and high drug delivery efficiency. In this review, we summarized the latest advances in the design and construction of different peptide-based hypoxia-targeting nanomaterials, including polypeptides, self-assembling peptides, and peptide-polymer conjugates, in addition to peptide functionalized liposomes and polysaccharides. The utilization of both peptide ligands and hypoxia-sensitive linkers, either together or apart, is the main strategy for targeting hypoxia. Through this strategy, peptide-based nanomaterials can be made to accumulate in hypoxic regions, target hypoxic cells and successfully deliver the payloads across biological barriers. In addition, these peptide-based nanomaterials can prolong blood circulation, improve permeability into angiogenic vessels and tumor tissues, and promote tumor cell uptake and therapeutic efficacy. Moreover, through intramolecular and intermolecular forces, peptides and their derivatives are easy to self-assemble into various nano-functional materials with different structures. These materials can take advantage of the unique characteristics of the hypoxic micro-environment or cancer cells, thereby improving the specificity of cancer cells. The literature provides strong evidence that the application of these peptide-based nanomaterials could improve the overall treatment efficiency of hypoxic diseases.

However, these studies are still in the preliminary stage. There are still several challenges preventing peptide-based nanomaterials from clinical application of hypoxic diseases. Peptides are easily degraded by enzymes and can be taken up by mononuclear phagocytes. Renal filtration also shortens the circulation time of peptides. Therefore, it is necessary to consider the system design and material modification of these peptide-based nanomaterials. More peptide ligands with new sequences need to be explored for specifically and efficiently targeting the hypoxic regions of different hypoxia diseases. Currently, many nanomaterials for medical applications are passively targeting tumor tissues through the enhanced permeability and retention (EPR) effect. Although the EPR effect can increase the enrichment of nanocarriers at the tumor site, poor cellular uptake and internalization limit the efficacy of chemotherapy. Therefore, it is necessary to combine peptides with various nanomaterials to construct a positive targeted multistage or multifunctional nanocomposite system to enhance cellular uptake and internalization, thereby enhancing the synergistic therapeutic effect of various therapies (PDT, photothermal therapy, thermodynamic therapy, chemotherapy,



radiotherapy, *etc.*) under hypoxic conditions. Critically, different hypoxia-related diseases such as tumors, bone tissue inflammation, cardiovascular diseases, and ischemic strokes all have specific hypoxic microenvironments, which requires rationally designed microenvironment-induced peptide-based materials for the treatment of these diseases according to the properties of peptides. In addition, the change in microenvironment *in vivo* could cause significant changes in the physicochemical properties of nanomaterials. Therefore, the biocompatibility, biodistribution, and *in vivo* targetability of these peptide-based nanomaterials should be evaluated in detail before clinical trials. We anticipate and look forward to the development of peptide-based hypoxia-targeting nanomaterials, as we believe they will make an important contribution to the progress in the diagnosis and treatment of hypoxia-related diseases in the near future.

## Conflicts of interest

There are no conflicts to declare.

## Acknowledgements

This work was financially supported by Teachers' Research of Jining Medical University (No. JYFC2018KJ068), the National Innovation Training Program for College Students (No. 201710443006), the PhD Scientific Research Start-up Fund of Jining Medical University, the Project of Shandong Province Higher Educational Science and Technology Program (No. J18KA093), and the Project of study abroad for excellent Young and middle-aged teachers sponsored by Jining Medical College. We thank Prof. Toshio Masuda and Dr Maocai Yan for assistance with English editing.

## Notes and references

- M. Li, J. Xia, R. Tian, J. Wang, J. Fan, J. Du, S. Long, X. Song, J. W. Foley and X. Peng, *J. Am. Chem. Soc.*, 2018, **140**, 14851–14859.
- L. Zhao, C. Fu, L. Tan, T. Li, H. Zhong and X. Meng, *Nanoscale*, 2020, **12**, 2855–2874.
- G. L. Semenza, *N. Engl. J. Med.*, 2011, **365**, 537–547.
- J. M. Brown and W. R. Wilson, *Nat. Rev. Cancer*, 2004, **4**, 437–447.
- H. Zhou, F. Qin and C. Chen, *Adv. Healthcare Mater.*, 2021, **10**, 2001277.
- W. R. Wilson and M. P. Hay, *Nat. Rev. Cancer*, 2011, **11**, 393–410.
- A. Dehsorkhi, V. Castelletto and I. W. Hamley, *J. Pept. Sci.*, 2014, **20**, 453–467.
- S. Wong, M. S. Shim and Y. J. Kwon, *J. Mater. Chem. B*, 2014, **2**, 595–615.
- S. Zhang, *Interface Focus*, 2017, **7**, 20170028.
- H. Sun, Y. Dong, J. Feijen and Z. Zhong, *J. Controlled Release*, 2018, **290**, 11–27.
- J. Zhao, Q. Li, X. Hao, X. Ren, J. Guo, Y. Feng and C. Shi, *J. Mater. Chem. B*, 2017, **5**, 8035–8051.
- J. S. Rudra, T. Sun, K. C. Bird, M. D. Daniels, J. Z. Gasiorowski, A. S. Chong and J. H. Collier, *ACS Nano*, 2012, **6**, 1557–1564.
- L. Zhang, Y. Huang, A. R. Lindstrom, T. Y. Lin, K. S. Lam and Y. Li, *Theranostics*, 2019, **9**, 7807–7825.
- D. Zhang, G. B. Qi, Y. X. Zhao, S. L. Qiao, C. Yang and H. Wang, *Adv. Mater.*, 2015, **27**, 6125–6130.
- A. N. Shirazi, D. Oh, R. K. Tiwari, B. Sullivan, A. Gupta, G. D. Bothun and K. Parang, *Mol. Pharmaceutics*, 2013, **10**, 4717–4727.
- S. Dissanayake, W. A. Denny, S. Gamage and V. Sarojini, *J. Controlled Release*, 2017, **250**, 62–76.
- Y. Gilad, E. Noy, H. Senderowitz, A. Albeck, M. A. Firer and G. Gellerman, *Bioorg. Med. Chem.*, 2016, **24**, 294–303.
- K. Xu, F. Wang, X. Pan, R. Liu, J. Ma, F. Kong and B. Tang, *Chem. Commun.*, 2013, **49**, 2554–2556.
- S. Xu, Q. Wang, Q. Zhang, L. Zhang, L. Zuo, J. D. Jiang and H. Y. Hu, *Chem. Commun.*, 2017, **53**, 11177–11180.
- Z. Yang, J. Cao, Y. He, J. H. Yang, T. Kim, X. Peng and J. S. Kim, *Chem. Soc. Rev.*, 2014, **43**, 4563–4601.
- T. Thambi, V. G. Deepagan, H. Y. Yoon, H. S. Han, S. H. Kim, S. Son, D. G. Jo, C. H. Ahn, Y. D. Suh, K. Kim, I. C. Kwon, D. S. Lee and J. H. Park, *Biomaterials*, 2014, **35**, 1735–1743.
- T. Thambi, S. Son, D. S. Lee and J. H. Park, *Acta Biomater.*, 2016, **29**, 261–270.
- J. Zheng, Y. Shen, Z. Xu, Z. Yuan, Y. He, C. Wei, M. Er, J. Yin and H. Chen, *Biosens. Bioelectron.*, 2018, **119**, 141–148.
- Y. Zhou, M. Maiti, A. Sharma, M. Won, L. Yu, L. X. Miao, J. Shin, A. Podder, K. N. Bobba, J. Han, S. Bhuniya and J. S. Kim, *J. Controlled Release*, 2018, **288**, 14–22.
- A. Shah, M. S. Malik, G. S. Khan, E. Nosheen, F. J. Iftikhar, F. A. Khan, S. S. Shukla, M. S. Akhter, H.-B. Kraatz and T. M. Aminabhavi, *Chem. Eng. J.*, 2018, **353**, 559–583.
- T. R. Pearce, K. Shroff and E. Kokkoli, *Adv. Mater.*, 2012, **24**, 3803–3822.
- Y. Liu, D. Li, J. X. Ding and X. S. Chen, *Chin. Chem. Lett.*, 2020, **31**, 3001–3014.
- Y. Ou, Z. H. Tang, L. Sun, H. Y. Yu, J. Li, M. H. Zhao and H. Xu, *Asian J. Pharm. Sci.*, 2018, **13**, 191–196.
- H. Yu, Z. Tang, D. Zhang, W. Song, Y. Zhang, Y. Yang, Z. Ahmad and X. Chen, *J. Controlled Release*, 2015, **205**, 89–97.
- C. Deng, J. Wu, R. Cheng, F. Meng, H.-A. Klok and Z. Zhong, *Prog. Polym. Sci.*, 2014, **39**, 330–364.
- L. A. Canalle, D. W. Lowik and J. C. van Hest, *Chem. Soc. Rev.*, 2010, **39**, 329–353.
- Z. Ahmad, S. X. Lv, Z. H. Tang, A. Shah and X. S. Chen, *J. Biomater. Sci., Polym. Ed.*, 2016, **27**, 40–54.
- W. Yin, M. Qiang, W. D. Ke, Y. Han, J. F. Mukerabigwi and Z. S. Ge, *Biomaterials*, 2018, **181**, 360–371.
- J. Deng, F. Liu, L. N. Wang, Y. An, M. Gao, Z. Wang and Y. J. Zhao, *Biomater. Sci.*, 2019, **7**, 429–441.
- J. C. Yu, C. G. Qian, Y. Q. Zhang, Z. Cui, Y. Zhu, Q. D. Shen, F. S. Ligler, J. B. Buse and Z. Gu, *Nano Lett.*, 2017, **17**, 733–739.



- 36 Y. Li, J. Ding, X. Xu, R. Shi, P. E. Saw, J. Wang, S. Chung, W. Li, B. M. Aljaeid, R. J. Lee, W. Tao, L. Teng, O. C. Farokhzad and J. Shi, *Nano Lett.*, 2020, **20**, 4857–4863.
- 37 J. Zhen, S. Tian, Q. Liu, C. Zheng, Z. Zhang, Y. Ding, Y. An, Y. Liu and L. Shi, *Biomater. Sci.*, 2019, **7**, 2986–2995.
- 38 P. Zhang, H. L. Yang, W. Shen, W. G. Liu, L. Chen and C. S. Xiao, *ACS Biomater. Sci. Eng.*, 2020, **6**, 2167–2174.
- 39 X. S. Sun, M.-S. Jang, Y. Fu, J. H. Lee, D. S. Lee, Y. Li and H. Y. Yang, *Mater. Sci. Eng., C*, 2020, **114**, 111069.
- 40 J. S. Suk, Q. Xu, N. Kim, J. Hanes and L. M. Ensign, *Adv. Drug Delivery Rev.*, 2016, **99**, 28–51.
- 41 E. Blanco, H. Shen and M. Ferrari, *Nat. Biotechnol.*, 2015, **33**, 941–951.
- 42 J. J. Li, X. Meng, J. Deng, D. Lu, X. Zhang, Y. R. Chen, J. D. Zhu, A. P. Fan, D. Ding, D. L. Kong, Z. Wang and Y. J. Zhao, *ACS Appl. Mater. Interfaces*, 2018, **10**, 17117–17128.
- 43 L. Zhao, Q. Zou and X. Yan, *Bull. Chem. Soc. Jpn.*, 2019, **92**, 70–79.
- 44 S. Lee, T. H. T. Trinh, M. Yoo, J. Shin, H. Lee, J. Kim, E. Hwang, Y.-b. Lim and C. Ryou, *Int. J. Mol. Sci.*, 2019, **20**, 5850.
- 45 Z. Feng, H. Wang, X. Chen and B. Xu, *J. Am. Chem. Soc.*, 2017, **139**, 15377–15384.
- 46 J. Wang, F. Shao, W. Li, J. Yan, K. Liu, P. Tao, T. Masuda and A. Zhang, *Chem. –Asian J.*, 2017, **12**, 497–502.
- 47 S. Yang, D. Xu and H. Dong, *J. Mater. Chem. B*, 2018, **6**, 7179–7184.
- 48 J. Boekhoven and S. I. Stupp, *Adv. Mater.*, 2014, **26**, 1642–1659.
- 49 S. H. Kim and J. R. Parquette, *Nanoscale*, 2012, **4**, 6940–6947.
- 50 N. Habibi, N. Kamaly, A. Memic and H. Shafiee, *Nano Today*, 2016, **11**, 41–60.
- 51 M. Ikeda, M. Kawakami and Y. Kitade, *Chem. Lett.*, 2015, **44**, 1137–1139.
- 52 C. R. Arnt, M. V. Chiorean, M. P. Heldebrant, G. J. Gores and S. H. Kaufmann, *J. Biol. Chem.*, 2002, **277**, 44236–44243.
- 53 M. J. Ernting, M. Murakami, A. Roy and S. D. Li, *J. Controlled Release*, 2013, **172**, 782–794.
- 54 W. W. Wang, X. Y. Li, Z. H. Wang, J. F. Zhang, X. Dong, Y. Z. Wu, C. Fang, A. W. Zhou and Y. L. Wu, *Nanoscale*, 2019, **11**, 2211–2222.
- 55 D. Guo, S. Xu, N. Wang, H. Jiang, Y. Huang, X. Jin, B. Xue, C. Zhang and X. Zhu, *Biomaterials*, 2017, **144**, 188–198.
- 56 B. Peng, X. Zhao, M. S. Yang and L. L. Li, *J. Mater. Chem. B*, 2019, **7**, 5626–5632.
- 57 H. Wang, Z. Feng and B. Xu, *Chem. Soc. Rev.*, 2017, **46**, 2421–2436.
- 58 T. B. Potocky, A. K. Menon and S. H. Gellman, *J. Am. Chem. Soc.*, 2005, **127**, 3686–3687.
- 59 J. Li, K. Shi, Z. F. Sabet, W. Fu, H. Zhou, S. Xu, T. Liu, M. You, M. Cao, M. Xu, X. Cui, B. Hu, Y. Liu, C. Chen, Z. F. Sabet and C. Chen, *Sci. Adv.*, 2019, **5**, eaax0937.
- 60 P. A. Taylor and A. Jayaraman, *Annu. Rev. Chem. Biomol. Eng.*, 2020, **11**, 257–276.
- 61 L. Milane, Z. Duan and M. Amiji, *Mol. Pharmaceutics*, 2010, **8**, 185–203.
- 62 H. S. Abyaneh, A. H. Soleimani, M. R. Vakili, R. Soudy, K. Kaur, F. Cuda, A. Tavassoli and A. Lavasanifar, *Pharmaceutics*, 2018, **10**, 196.
- 63 A. Vasconcelos, E. Vega, Y. Perez, M. J. Gomara, M. L. Garcia and I. Haro, *Int. J. Nanomed.*, 2015, **10**, 609–631.
- 64 T. Teesalu, K. N. Sugahara and E. Ruoslahti, *Front. Radiat. Oncol.*, 2013, **3**, 216.
- 65 H. Liu, W. Jiang, Q. Wang, L. Hang, Y. Wang and Y. Wang, *Biomater. Sci.*, 2019, **7**, 3706–3716.
- 66 N. Dube, J. W. Seo, H. Dong, J. Y. Shu, R. Lund, L. M. Mahakian, K. W. Ferrara and T. Xu, *Biomacromolecules*, 2014, **15**, 2963–2970.
- 67 H. Sun, Y. Hong, Y. Xi, Y. Zou, J. Gao and J. Du, *Biomacromolecules*, 2018, **19**, 1701–1720.
- 68 P. Kulkarni, M. K. Haldar, F. Karandish, M. Confeld, R. Hossain, P. Borowicz, K. Gange, L. Xia, K. Sarkar and S. Mallik, *Chemistry*, 2018, **24**, 12490–12494.
- 69 B. Mamnoon, J. Loganathan, M. I. Confeld, N. De Fonseca, L. Feng, J. Froberg, Y. Choi, D. M. Tuvin, V. Sathish and S. Mallik, *ACS Appl. Bio Mater.*, 2021, **4**, 1450–1460.
- 70 D. Ma, C. Huang, J. Zheng, W. Zhou, J. Tang, W. Chen, J. Li and R. Yang, *Anal. Chem.*, 2019, **91**, 1360–1367.
- 71 K. M. Ihsanullah, B. N. Kumar, Y. Zhao, H. Muhammad, Y. Liu, L. Wang, H. Liu and W. Jiang, *Biomaterials*, 2020, **245**, 119982.
- 72 C. Y. Zhao, Y. J. Tong, X. L. Li, L. H. Shao, L. Chen, J. Q. Lu, X. W. Deng, X. Wang and Y. Wu, *Small*, 2018, **14**, 1703045.
- 73 N. Song, L. Zhao, X. Xu, M. Zhu, C. Liu, N. Sun, J. Yang, X. Shi and J. Zhao, *ACS Appl. Mater. Interfaces*, 2020, **12**, 12395–12406.
- 74 Z. Zhang, W. Yang, F. Ma, Q. Ma, B. Zhang, Y. Zhang, Y. Liu, H. Liu and Y. Hua, *Drug Delivery*, 2020, **27**, 691–702.
- 75 V. Cicatiello, I. Apicella, L. Tudisco, V. Tarallo, L. Formisano, A. Sandomenico, Y. Kim, A. Orlandi, J. Ambati, M. Ruvo, R. Bianco and S. D. Falco, *Oncotarget*, 2015, **6**, 10563–10576.
- 76 R. Cheng, L. Liu, Y. Xiang, Y. Lu, L. Deng, H. Zhang, H. A. Santos and W. Cui, *Biomaterials*, 2020, **232**, 119706.
- 77 A. Gonzalez Gomez and Z. Hosseinidoust, *ACS Infect. Dis.*, 2020, **6**, 896–908.
- 78 A. Akbarzadeh, R. Rezaei-Sadabady, S. Davaran, S. W. Joo, N. Zarghami, Y. Hanifehpour, M. Samiei, M. Kouhi and K. Nejati-Koshki, *Nanoscale Res. Lett.*, 2013, **8**, 102.
- 79 K. S. Ahmed, S. A. Hussein, A. H. Ali, S. A. Korma, Q. Lipeng and C. Jinghua, *J. Drug Targeting*, 2019, **27**, 742–761.
- 80 S. Zununi Vahed, R. Salehi, S. Davaran and S. Sharifi, *Mater. Sci. Eng., C*, 2017, **71**, 1327–1341.
- 81 C. Yu-Wai-Man, A. D. Tagalakakis, M. D. Manunta, S. L. Hart and P. T. Khaw, *Sci. Rep.*, 2016, **6**, 21881.
- 82 A. D. Tagalakakis, L. He, L. Saraiva, K. T. Gustafsson and S. L. Hart, *Biomaterials*, 2011, **32**, 6302–6315.
- 83 A. A. Kale and V. P. Torchilin, *J. Liposome Res.*, 2007, **17**, 197–203.
- 84 Y. T. Ko, W. C. Hartner, A. Kale and V. P. Torchilin, *Gene Ther.*, 2009, **16**, 52–59.



- 85 Y. Wang, M. Fu, J. Liu, Y. Yang, Y. Yu, J. Li, W. Pan, L. Fan, G. Li, X. Li and X. Wang, *Int. J. Nanomed.*, 2019, **14**, 4071–4090.
- 86 P. Kulkarni, M. K. Haldar, P. Katti, C. Dawes, S. You, Y. Choi and S. Mallik, *Bioconjugate Chem.*, 2016, **27**, 1830–1838.
- 87 Y. Dai, B. Wang, Z. Sun, J. Cheng, H. Zhao, K. Wu, P. Sun, Q. Shen, M. Li and Q. Fan, *ACS Appl. Mater. Interfaces*, 2019, **11**, 39410–39423.
- 88 Y. Wang, Y. Xie, J. Li, Z. H. Peng, Y. Sheinin, J. Zhou and D. Oupicky, *ACS Nano*, 2017, **11**, 2227–2238.
- 89 W. Li, J. Yang, L. Luo, M. Jiang, B. Qin, H. Yin, C. Zhu, X. Yuan, J. Zhang, Z. Luo, Y. Du, Q. Li, Y. Lou, Y. Qiu and J. You, *Nat. Commun.*, 2019, **10**, 3349.
- 90 R. B. P. Elmes, *Chem. Commun.*, 2016, **52**, 8935–8956.
- 91 Q. Yang, S. Wang, D. Li, J. Yuan, J. Xu and S. Shao, *Anal. Chim. Acta*, 2020, **1103**, 202–211.
- 92 C. Zhu, Z. Zou, C. Huang, J. Zheng, N. Liu, J. Li and R. Yang, *Chem. Commun.*, 2019, **55**, 3235–3238.
- 93 Y. Fan, M. Lu, X. A. Yu, M. He, Y. Zhang, X. N. Ma, J. Kou, B. Y. Yu and J. Tian, *Anal. Chem.*, 2019, **91**, 6585–6592.
- 94 Y. Yao, L. Feng, Z. Wang, H. Chen and N. Tan, *Biomater. Sci.*, 2020, **8**, 256–265.
- 95 J. H. Xie, M. L. Jin, G. A. Morris, X. Q. Zha, H. Q. Chen, Y. Yi, J. E. Li, Z. J. Wang, J. Gao, S. P. Nie, P. Shang and M. Y. Xie, *Crit. Rev. Food Sci. Nutr.*, 2016, **56**(1), S60–S84.
- 96 M. Swierczewska, H. S. Han, K. Kim, J. H. Park and S. Lee, *Adv. Drug Delivery Rev.*, 2016, **99**, 70–84.
- 97 M. Li, F. Lin, Y. Lin and W. Peng, *Biochem. Biophys. Res. Commun.*, 2015, **466**, 748–754.
- 98 B. Laha, S. Maiti, K. K. Sen and S. Jana, in *Green Synthesis, Characterization and Applications of Nanoparticles*, Elsevier, 2019, pp. 347–368.
- 99 S. W. Shin, W. Jung, C. Choi, S. Y. Kim, A. Son, H. Kim, N. Lee and H. C. Park, *Mar. Drugs*, 2018, **16**, 510.
- 100 S. Uthaman, Y. Kim, J. Y. Lee, S. Pillarisetti, K. M. Huh and I. K. Park, *ACS Appl. Mater. Interfaces*, 2020, **12**, 28004–28013.
- 101 W. Park, B. C. Bae and K. Na, *Biomaterials*, 2016, **77**, 227–234.
- 102 C. Zhang, Q. Li, C. Wu, J. Wang, M. Su and J. Deng, *Nanotechnology*, 2021, **32**, 095107.
- 103 Y. Shu, T. Hao, F. Yao, Y. Qian, Y. Wang, B. Yang, J. Li and C. Wang, *ACS Appl. Mater. Interfaces*, 2015, **7**, 6505–6517.
- 104 G. Ghalamfarsa, M. H. Kazemi, S. Raoofi Mohseni, A. Masjedi, M. Hojjat-Farsangi, G. Azizi, M. Yousefi and F. Jadidi-Niaragh, *Expert Opin. Ther. Targets*, 2019, **23**, 127–142.
- 105 F. Hajizadeh, S. Moghadaszadeh Ardebili, M. Baghi Moornani, A. Masjedi, F. Atyabi, M. Kiani, A. Namdar, V. Karpisheh, S. Izadi, B. Baradaran, G. Azizi, G. Ghalamfarsa, G. Sabz, M. Yousefi and F. Jadidi-Niaragh, *Eur. J. Pharmacol.*, 2020, **882**, 173235.
- 106 Y. Zhou, B. Yang, X. Ren, Z. Liu, Z. Deng, L. Chen, Y. Deng, L. M. Zhang and L. Yang, *Biomaterials*, 2012, **33**, 4731–4740.
- 107 L. Deng, F. Zhang, Y. Wu, J. Luo, X. Mao, L. Long, M. Gou, L. Yang and D. Y. B. Deng, *ACS Biomater. Sci. Eng.*, 2019, **5**, 6254–6264.

